

Published in final edited form as:

*Diabetologia*. 2010 August ; 53(8): 1656–1668. doi:10.1007/s00125-010-1733-9.

## Beta cell specific ZnT8 deletion in mice causes marked defects in insulin processing, crystallization and secretion

N. Wijesekara<sup>#1</sup>, F.F. Dai<sup>#1</sup>, A.B. Hardy<sup>#1</sup>, P. R. Giglou<sup>1</sup>, A. Bhattacharjee<sup>1</sup>, V. Koshkin<sup>1</sup>, F. Chimienti<sup>3</sup>, H.Y. Gaisano<sup>1,2</sup>, G.A. Rutter<sup>4</sup>, and M.B. Wheeler<sup>1,2</sup>

<sup>1</sup>Department of Physiology, University of Toronto, Toronto, Canada <sup>2</sup>Department of Medicine, University of Toronto, Toronto, Canada <sup>3</sup>Mellitech, Grenoble, France <sup>4</sup>Section of Cell Biology, Division of Medicine, Imperial College London, London, England

# These authors contributed equally to this work.

### Abstract

**Aims/hypothesis**—Zinc is highly concentrated in pancreatic beta cells, is critical for normal insulin storage, and may regulate glucagon secretion from alpha cells. ZnT8 is a zinc efflux transporter highly expressed in beta cells and polymorphisms in the ZnT8 (*slc30a8*) gene in man are associated with increased risk of type 2 diabetes. Whilst global ZnT8 knockout (ZnT8KO) mice have been characterized, ZnT8 is also expressed in other islet cell types and extra-pancreatic tissues. Therefore, it is important to devise strategies to understand the role of ZnT8 in beta and alpha cells without the confounding effects of ZnT8 in these other tissues.

**Methods**—We have generated beta and alpha cell specific ZnT8 knockout (ZnT8BKO and ZnT8AKO) mice and performed *in vivo* and *in vitro* characterization of the phenotypes to determine the functional and anatomical impact of ZnT8 in these cells. Thus we assessed zinc accumulation, insulin granule morphology, insulin biosynthesis and secretion, and glucose homeostasis.

**Results**—ZnT8BKO mice are glucose intolerant, have reduced beta cell zinc accumulation and atypical insulin granules. They also display reduced first phase glucose-stimulated insulin secretion, reduced insulin processing enzyme transcripts and increased proinsulin levels. In contrast, ZnT8AKO mice show no evident abnormalities in plasma glucagon and glucose homeostasis.

**Conclusion/interpretation**—We provide the first report of specific beta and alpha cell deletion of ZnT8. Our data indicate that while ZnT8 is absolutely required for proper beta cell function, under the conditions studied, it is largely dispensable for alpha cell function.

### Keywords

ZnT8; *slc30a8*; Beta Cell; Alpha Cell; Pancreatic Islets; Insulin; Glucagon; Zinc

---

**Address correspondence to:** M. B. Wheeler, Department of Physiology, University of Toronto, 1 King's College Circle Room 3352, Toronto, ON, Canada M5S 1A8, michael.wheeler@utoronto.ca, Tel.: +1-416-9786737, Fax: +1-416-9784940.

**Conflict of Interest.** GAR has received grant support from Servier IdS (France). FC is employed by Mellitech (France).

## Introduction

ZnT8 (*SLC30A8*) is a member of the cation diffusion facilitator family and a zinc efflux transporter recently linked to type 2 diabetes [1–5]. Since then, ZnT8 was also found to be targeted by auto-antibodies in type 1 diabetic patients [6]. Interestingly, studies suggest that the risk allele of ZnT8 is associated with reduced insulin secretion in type 2 diabetics [7, 8]. The important role of zinc in modulating insulin biosynthesis and secretion [9] and the unique localization of ZnT8 with insulin [10, 11], has channelled much interest towards determining the function of ZnT8 in controlling glucose homeostasis.

The generation of global ZnT8 knockout (ZnT8KO) mice has provided an excellent tool to better study the link between diabetes and ZnT8. These mice are glucose intolerant with abnormalities in zinc accumulation, insulin granule morphology and insulin secretion from beta cells [12–14], although some differences in phenotypes exist between groups. Interestingly, on a high fat diet, ZnT8KO mice were severely insulin resistant and more obese than controls, suggesting that ZnT8 may play a role in peripheral tissues. Thus, glucose intolerance may not necessarily result from the absence of ZnT8 in beta cells alone. Although ZnT8 was originally thought to be pancreas specific [11, 15], studies now suggest its expression in human adipose tissue [16], blood lymphocytes [17], and the cubical epithelium that lines thyroid follicles and adrenal cortex [18]. Furthermore, we have shown that ZnT8 is also expressed in alpha cells [13, 19]. However, its function there remains unknown since glucagon is not thought to require zinc for processing and packaging although zinc is localised to alpha cell granules [20]. Interestingly, a recent study showed that over-expression of ZnT8 inhibits, while knockdown stimulates glucagon secretion in cultured mouse alpha cells [21], suggesting that glucagon secretion may be regulated directly by ZnT8, thus indirectly affecting insulin secretion. It is therefore important to devise strategies to understand the role of ZnT8 in beta cells without the confounding effects from other tissues including alpha cells. Moreover, the insights gained from such studies may also begin to explain the marked phenotypic differences between different colonies of ZnT8KO mice [12–14]. Finally, as some [19, 22–24] though not all [13, 25] previous studies suggest that glucagon secretion might be regulated by zinc released from beta cells, it is also important to study the impact of ZnT8 on alpha cell function.

In this study, we have generated both beta (ZnT8BKO) and alpha (ZnT8AKO) cell specific ZnT8 knockout mouse models. We show that ZnT8BKO mice are glucose intolerant with reduced beta cell zinc accumulation, abnormal beta cell granule morphology and impaired insulin processing. Furthermore, reduced first phase insulin response to glucose was evident compared to controls suggesting impaired insulin secretion. In contrast, ZnT8AKO mice show no visible phenotypic differences compared to control mice.

## Materials and Methods

### Generation of cell-specific ZnT8 knockout mice

Chimeric males were bred with C57Bl/6J wild-type mice to generate heterozygous mice carrying the floxed allele. These animals were then mated with pCAG-Flp-expressing C57Bl/6J mice to excise the FRT flanked neomycin cassette and generate neomycin-excised

conditional ZnT8 mice (ZnT8loxP). The loxP sites flank exon 1 which contains the start codon for ZnT8 and thus homozygous mice crossed to cell specific *Cre* mice lack ZnT8 in that cell type (Figure 2a). ZnT8loxP mice were obtained from Genoway, France. **ZnT8BKO:** ZnT8loxP mice were crossed to Rat Insulin Promoter (RIP)-*Cre* mice. Since RIP promoter can also drive deletion in the hypothalamus [26], ZnT8 expression was determined in this tissue: low, though detectable, ZnT8 expression was apparent by quantitative PCR (qPCR) analysis (Figure 2c). **ZnT8AKO:** ZnT8loxP mice were crossed to glucagon promoter (Gcg)-*Cre*-ROSA26EYFP (Gcg-*Cre*-YFP) mice [27]. This cross allows labelling of alpha cells with YFP where *Cre* is expressed. Mice were genotyped using tail DNA and standard multiplex PCR using *flox* and *Cre* primers (Suppl Table 1) (Figure 2b). Mice expressing *Cre* transgene alone were used as controls (RIP-*Cre* mice were controls for ZnT8BKO mice and Gcg-*Cre*-YFP mice were controls for ZnT8AKO mice) and male 6-8 week old mice were used for all experiments, unless otherwise mentioned. All experiments were approved by the Animal Care Committee at the University of Toronto and animals were handled according to the guidelines of the Canadian Council of Animal Care.

### Islet isolation and dispersion

Mouse islets were isolated by collagenase digestion of the mouse pancreas and dispersed as described [28]. Human islets isolated following the Edmonton Protocol [29] from healthy donors were provided by James Shapiro and the ABCC Human Islet Distribution Program at the University of Alberta. Human islets were dispersed as described [30].

### Transmission electron microscopy (TEM)

Islets were prepared and images were acquired as described [13]. Dense core, empty, light core (gray) and atypical (rod-shaped) granules were manually counted and quantified.

### Immunogold-cryo electron microscopy

Cryo-electron microscopy and immunogold labelling of ZnT8 was performed as described [31]. Based on insulin and glucagon immuno-gold labelling and literature on granule characterization [32], cells within the center of the mouse islet with granules containing a dense core and a large translucent halo were identified as beta cells, while peripheral cells of the mouse islet with granules containing a dense core and a thin rim halo were identified as alpha cells. Human beta cells were identified strictly by the large translucent halo.

### Western immuno-blot analysis

Western blot analysis was performed as described [13]. Lysates were resolved by 10% SDS-PAGE and immunoblotted with polyclonal anti-ZnT8 (1:500; Mellitech, Grenoble, France) or anti-beta actin (1:2000) antibodies followed by anti-rabbit secondary antibody from Sigma, St. Louis, MO, USA. Immunoblots were scanned on a Kodak imager within the linear range of intensity.

### Quantitative real time PCR

qPCR analysis was performed as described [19, 30]. Primers are listed in Suppl Table 1. Data were normalized to mouse beta actin mRNA.

### Immunostaining and confocal microscopy

Dispersed islet cells were fixed in 4% paraformaldehyde for 15 min, permeabilized with 2% triton-X-100 for 10 min and blocked overnight in 5% BSA at 4°C. Cells were then labelled with polyclonal anti-ZnT8 (1:300) and anti-insulin (DAKO, Glostrup, Denmark), monoclonal anti-glucagon (1:300, Sigma, St. Louis, MO, USA) and anti-gfp (1:300, Santa Cruz Biotechnology Inc., Santa Cruz, CA, USA) antibodies overnight at 4°C and stained at room temperature for 30 min with Cy5-conjugated anti-rabbit, FITC-conjugated anti-guinea pig or FITC-conjugated anti-mouse secondary antibodies (Jackson ImmunoResearch Laboratories Inc., West Grove, PA, USA) respectively [13, 19]. Cells were washed and mounted on glass slides. Images were acquired using Zeiss LSM510 software on a confocal microscope using 488/633 nm excitation laser line and 545 nm beam-splitter.

### Oral glucose tolerance test (OGTT)

Following a 6 h fast, glucose (1.5 g/kg body weight) was given by oral gavage and blood glucose was measured at 0, 10, 20, 30, 60, 120 min from tail vein blood using a glucometer. Blood was collected at 0, 10, 30, 60 and 120 min from the tail vein in EDTA coated microvettes (Sarstedt AG & Co., Nümbrecht, Germany) for insulin and at 0 and 10 min for proinsulin measurements. Area under the curve was calculated using Graph Pad Prism software. Homeostatic model assessment for insulin resistance (HOMA-IR) index was calculated at fasting, using the following formula:  $\text{HOMA-IR} = \text{fasting glucose (mmol/L)} \times \text{fasting insulin } (\mu\text{U/mL})/22.5$ .

### Glucagon, insulin and proinsulin measurements

Blood was collected from 16 h fasted mice from tail vein for glucagon measurements. Plasma was separated from whole blood by centrifugation at 8000 rpm for 10 min. Plasma insulin, and islet and plasma proinsulin were measured using ELISA kits from ALPCO diagnostics (Salem, NH, USA) and Mercodia (Uppsala, Sweden) respectively. Proinsulin detection was performed per manufacturer's instructions: Proinsulin in the sample reacts with anti-proinsulin antibodies bound to microtitration wells and peroxidase-conjugated antibodies in the solution. The bound conjugate is detected by reaction with 3,3',5,5' tetramethylbenzidine. The kit detects proinsulin I and II. Islet insulin content and plasma glucagon were measured by radioimmunoassay kits from Linco Research (Millipore Corp., Billerica, MA, USA).

### Islet morphological analysis

Isolated pancreata were prepared and labelled for insulin and glucagon as described [28]. Slides were digitized on a bright-field scanner at 20 times magnification and analyzed using ImageScope software (Aperio Technologies, Vista, CA, USA) using the positive-pixel count algorithm. Results were normalized to whole slice area (total pixel count). Beta and alpha cell mass was determined using the total pancreatic weight. Islet number per slice was manually counted and normalized to whole slice area. For islet size measurements, images were acquired on confocal microscope using Zeiss LSM510 software at 20 times magnification and subsequently, area of each islet was calculated using Aperio ImageScope software.

### Zinc content measurement

Cell zinc content was measured using Zinquin (Mellitech, Grenoble, France) as described [13, 33].

### Insulin secretion

Insulin secretion was assessed by islet perfusion as described [30]. Area under the curve was calculated using Graph Pad Prism software.

### Statistical analysis

One-way repeated measures ANOVA with Tukey-Kramer or Bonferroni's post-hoc test was used to analyze OGTT and islet perfusion experiments and determine significant variation in insulin secretion and blood glucose levels. In all other experiments, Student's *t* test was used.  $P < 0.05$  was considered statistically significant. Data are expressed as mean  $\pm$  SEM. The N number represents the number of animals used.

## Results

### ZnT8 is expressed in granules of beta and alpha cells

Co-staining for ZnT8 and insulin/glucagon in mouse islets reiterates our previous findings that ZnT8 is expressed in both beta and alpha cells (Figure 1a) [12–14, 19]. Not all dispersed cells were stained for ZnT8 (Suppl. Figure 1) and based on previous studies, these cells may be delta cells [19, 34]. Furthermore, we have shown in Nicolson *et al* that ZnT8 immunoreactivity is also absent in acinar cells [13]. Such immunostaining studies so far have been the only means to suggest localization of ZnT8 to insulin granules [10, 13] and ultrastructural localization of ZnT8 in alpha cells is currently unknown. We confirm here using TEM that ZnT8 is indeed localized within the granules of both mouse and human beta cells (Figure 1b, Suppl Figure 2) as well as in non-beta cells (Suppl Figure 2) which we suggest to be alpha cells.

### Reduced ZnT8 expression in ZnT8BKO mice

The expression of ZnT8 in islets was significantly reduced in ZnT8BKO mice, determined by western immuno-blot (Figure 2d) and qPCR (Figure 2e) analysis. The latter revealed approximately 90% reduction in ZnT8 mRNA in ZnT8BKO islets compared to controls. Immunostaining experiments showed that dispersed islet cells positive for insulin in ZnT8BKO mice were negative for ZnT8 (Figure 2f). Those negative for insulin were positive for ZnT8. Conversely, in control islets, all insulin-positive cells were positive for ZnT8. This shows selective ZnT8 deletion in beta cells of ZnT8BKO islets. Further, qPCR analysis indicates no compensatory changes in the expression of other ZnT isoforms (Figure 2g) or  $Ca_v1.1$ , 1.2 and 1.3 subunits forming L-type calcium channels (Suppl Figure 3), which also contribute to zinc transport in beta cells [33].

### ZnT8BKO mice are glucose intolerant

We have previously shown that male ZnT8KO mice are mildly hyperglycaemic and glucose intolerant as early as six weeks of age [13], while others have shown normal glucose

homeostasis up to 1 year of age [12, 14]. The current study shows that ZnT8BKO mice have similar body weights (Figure 3a) and fasting blood glucose (Figure 3b) compared to control mice, but are glucose intolerant (as measured by the area under the OGTT curve) (Figure 3c) also as early as six weeks of age. Interestingly, plasma insulin measurements during the OGTT showed no difference between groups (Figure 3d). HOMA-IR indices (measurement of insulin resistance) were therefore also similar in control and ZnT8BKO mice ( $3.32 \pm 0.55$  and  $3.71 \pm 0.54$  respectively).

### **ZnT8BKO mice show abnormal beta cell morphology, reduced islet insulin processing and beta cell zinc accumulation**

Islet morphological analysis revealed that restricting ZnT8 knockdown to beta cells had no effect on islet architecture, showing no clear differences in islet size (Figure 4a), islet number (Figure 4b), beta cell mass (Figure 4c) or alpha cell mass (Figure 4d) between ZnT8BKOs and controls. In contrast, beta cell granule morphology was significantly altered in these mice compared to controls. We observed a reduction in the total number of granules and dense core granules per given area, with a subsequent increase in the number of empty, light core (gray) and atypical (rod-shaped) granules in beta cells from ZnT8BKO mice (Figure 4e) suggesting defective insulin crystallization and packaging.

Interestingly, ZnT8BKO mice had significantly more plasma proinsulin in both fed and fasting conditions, while plasma insulin levels were unaltered (Figure 5a-b). Similarly, proinsulin content in ZnT8BKO islets was also increased compared to controls (Figure 5c) suggesting defective insulin processing in these mice. Furthermore, mRNA expression of transcription factors, *Pdx1* and *MafA*, and processing enzymes, *prohormone convertase 1 and 2 (PC1 and PC2)* and *carboxypeptidase E (CpE)* involved in insulin biosynthesis were reduced in ZnT8BKO islets compared to controls, although *Insulin 1 and 2 (INS1 and INS2)* mRNA was only slightly reduced (Figure 5d-e). Interestingly, *kcnj11*, KATP channel gene expression was also reduced in ZnT8BKO mice. Static zinc content measurements also revealed a reduction in zinc accumulation in dispersed islet cells from ZnT8BKO mice compared to controls (Figure 6a).

### **ZnT8BKO mice show a reduced first phase insulin response**

When isolated islets were perfused with low (2.8 mM) and high (11 mM) glucose or 10 mM arginine (Figure 6b), we observed reduced first phase insulin secretion from ZnT8BKO islets compared to controls (as measured by the area under the OGTT curve). Both the second phase insulin secretion and the response to arginine were not significantly different between groups.

### **ZnT8AKO mice maintain normal plasma glucagon and glucose homeostasis**

Immunostaining for ZnT8 and YFP showed that dispersed islet cells positive for YFP in ZnT8AKO mice were negative for ZnT8, indicating that alpha cells expressing *Cre* recombinase lacked ZnT8 expression (Figure 7a). 76% of alpha cells were previously found to express YFP [27]. However, ZnT8AKO mice showed no evidence of glucose homeostasis abnormalities. Body weight gain (Figure 7b), fasting plasma glucagon levels (Figure 7c),

glucose tolerance (Figure 7d) and plasma insulin levels (Figure 7e) were similar in ZnT8AKO and control mice.

## Discussion

ZnT8 has recently attracted much attention after the identification in genome wide array studies of an association between a non-synonymous polymorphism in the *slc30a8* (ZnT8) gene and increased risk of type 2 diabetes [1–5]. Although immuno-fluorescent co-staining has localized ZnT8 with insulin [10, 11], our study is the first to demonstrate this at the level of the granule using TEM. Furthermore, although ZnT8 expression has been observed in alpha cells using immunostaining [12–14, 19] and qPCR analysis of highly purified primary mouse islet alpha cells [13], the subcellular localization of the protein has remained uncertain. We provide evidence here that ZnT8 also resides within glucagon granules. In support of a role for zinc in glucagon processing or packaging, recent studies by Egefjord and colleagues show zinc concentrated in the alpha cell secretory granule periphery [20].

Until its link to diabetes was established, only a couple of studies had explored the role of ZnT8 in beta cells. These suggested that ZnT8 over-expression increases, while knockdown decreases zinc accumulation and insulin secretion in cultured beta cells [10, 35]. Since then, three independent groups have studied ZnT8KO mice in order to understand the molecular link between ZnT8 and glucose homeostasis [12–14]. Although a significant loss of islet or beta cell zinc content was observed in all three studies, only Nicolson *et al.* reported significant glucose intolerance at most ages and in both sexes of ZnT8KO mice and decreased insulin secretion during intraperitoneal glucose tolerance test [13]. More importantly, the impact of ZnT8 deletion on *in vitro* insulin secretion had been variable [12–14] as Lemaire *et al.* [12] showed no effect, Pound *et al.* [14] showed a decrease, while Nicolson *et al.* [13] showed enhanced insulin secretion from ZnT8KO islets. While pancreatic or islet insulin content was unchanged in all three studies, Pound *et al.* [14] showed reduced fasting plasma insulin in ZnT8KO mice in contrast to the other two which showed no change [12, 13].

These differences have been attributed to possible variations in genetic background, age and diet of the mice [36]. We have now created the ZnT8BKO mice to provide a more appropriate model to understand ZnT8 specifically in the beta cell. The key findings in ZnT8BKO mice are glucose intolerance, reduced beta cell zinc accumulation and atypical insulin granules. *In vitro*, we demonstrate reduced first phase glucose-stimulated insulin secretion in ZnT8BKO mice, although plasma insulin was similar during OGTT between groups. Reasons for these differences remain unclear and require further investigation.

Our findings are in part consistent and inconsistent with the whole body ZnT8KO phenotype [12–14]. Since ZnT8 expression is not restricted to the beta cell [16–18], differences in glucose homeostasis between ZnT8KO and ZnT8BKO mice could be due to ZnT8 deletion in other cell types and compensatory changes at these sites. ZnT8 is expressed in the alpha cell, adipose tissue and the adrenal cortex, which are well known sites for the regulation of glucose homeostasis [37–39]. It is also possible that low but significant expression of ZnT8

centrally, including the hypothalamus, may also influence the activity of neurons involved in the control of feeding and satiety, or other aspects of energy homeostasis.

The mechanistic role of zinc in insulin biosynthesis has long been mapped out (Figure 8a-based on [40]). Briefly, transcription of the *Insulin* gene is mediated via the binding of transcription factors to conserved 5'-flanking region regulatory elements [41, 42]. Insulin, once translated, is directed into the endoplasmic reticulum as a single-chain molecule from which a signal peptide is cleaved forming proinsulin [40]. Proinsulin is then transferred to the Golgi apparatus, an environment rich in zinc. Other studies show that ZnT5 is expressed in the Golgi and may be the primary transporter to move zinc into this organelle [43]. Zinc-proinsulin hexamerization occurs here, introducing two zinc ions into each hexamer [40]. Proinsulin to insulin conversion occurs during vesicle formation and is facilitated by prohormone convertases and carboxypeptidases [40, 44, 45]. Importantly, insulin crystallization occurs within insulin granules, forming dense cores, in a process that requires up to 11.6 zinc ions per insulin hexamer [9]. Our data indicate that ZnT8 is localized to insulin granules (Figure 1b) and represents the primary transporter to move zinc into these organelles and is necessary for proper insulin crystallization. Without ZnT8, zinc transport is reduced and dense core granules rarely form (Figure 4e and 6a).

The significant reduction in insulin granule crystallization leading to less dense core granules is reminiscent of beta cells from animals with deficiencies in insulin processing enzymes [46, 47] (see Figure 8a). In addition to crystallization, the increased presence of empty granules seen in ZnT8BKO beta cells suggests a general defect in insulin packaging. Increased plasma and islet proinsulin, and reduced expression of key transcription factors and insulin processing enzyme genes in ZnT8BKO mice suggest defects in both insulin transcription and processing (Figure 8). As zinc is an important co-factor for gene transcription, this reduction in expression of *Pdx1* and *MafA* and processing enzymes could be a general phenomenon of zinc deficiency in beta cells. There are in fact a number of zinc dependent transcription factors known to regulate PDX1 and MafA which could affect *Insulin* gene expression [48, 49]. As such, we observed a trend towards reduced *Insulin* gene expression, but surprisingly failed to observe a corresponding decrease in plasma insulin, which may have been due to the inability of current methods to differentiate between proinsulin, insulin or other inactive forms. However, the more remarkable reduction in the expression of proinsulin converting enzyme genes indicates that the principle impact is on post-translational modifications in the insulin biosynthetic pathway. The impairment in proinsulin to insulin conversion has also been observed in human carriers of ZnT8 risk allele [50]. *In vitro*, ZnT8BKO islets displayed reduced first phase insulin secretion which could be due to reduced cargo or from the reduced or delayed exocytosis of insulin granules (Figure 8). Both scenarios are supported in the present study. First, indiscriminate exocytosis of granules regardless of maturity or crystallization status including empty granules would lead to reduced insulin secretion. In addition, ZnT8BKO beta cells contain fewer granules per given area compared to control cells. Second, a zinc deficiency in ZnT8BKO islets could affect the activity of zinc-dependent transcription factors and proteins associated with glucose sensing and the exocytotic machinery. For example, a decrease in the expression of the *kcnj11* gene encoding the KATP channel subunit Kir 6.2, as observed here could affect glucose responsiveness. Future studies will investigate these possibilities further.



Previously it has been shown that zinc regulates glucagon secretion from alpha cells [19, 22–24] however this is not a universal finding in the literature [13, 25, 39] and the mechanism of inhibition is still a matter of debate. Based on evidence that zinc inhibits glucagon secretion and that zinc and ZnT8 are localized to the alpha cell granule [20], we would predict an increase in glucagon secretion from alpha cells lacking ZnT8 specifically. Alternatively, since ZnT8 is localized to the glucagon granules, its deletion might cause zinc accumulation within the cytosol and thus, suppression of glucagon secretion in this way. Regardless of the possible method, in the present study, we observed no differences in fasting plasma glucagon levels in ZnT8AKO and control mice and no differences in glucose homeostasis. Thus, under the conditions studied, ZnT8 appears largely dispensable for alpha cell function. Further examination of ZnT8AKO islets and isolated alpha cells however may reveal important physiological functions of zinc and ZnT8 in this cell type.

In conclusion, we provide the first report of specific beta and alpha cell deletion of ZnT8. Our study suggests that ZnT8 does not have a major role in glucagon biosynthesis and secretion. In contrast, we demonstrate that ZnT8 is absolutely required for proper insulin processing, crystallization and packaging and this, in turn, is a requirement for maintaining normal insulin secretion and glucose homeostasis (Figure 8b). The similarities between the phenotypes of ZnT8KO and ZnT8BKO mice makes it apparent that the phenotype of the former is indeed primarily a consequence of ZnT8 deletion in beta cells and not alpha cells or other sites of ZnT8 activity, while the differences may have arisen due to compensation at these other sites in ZnT8KO mice. Interestingly, the ZnT8BKO phenotype which has remarkably similar characteristics to human carriers of the risk allele of ZnT8 [7, 8, 50] suggests that these mouse models can bring us even closer to understand the molecular mechanisms linking ZnT8 variants to the development of type 2 diabetes.

## Supplementary Material

Refer to Web version on PubMed Central for supplementary material.

## Acknowledgements

This work was supported by a grant from the Canadian Institutes of Health Research (CIHR) (MOP49521 and MOP12898) to MBW. A doctoral award from CIHR supported NW. GAR was supported by Programme and Project grants from the Wellcome Trust, National Institutes of Health, Medical Research Council (UK), Juvenile Diabetes Research Foundation International, Diabetes UK and the European Union. We thank Dr. Pedro Herrera and Dr. Patrick Gilon for kindly providing the Gcg-*Cre*-YFP mice. RIP-*Cre* mice were generously given by Dr. Minna Woo. We also thank Robert Temkin (Advanced Bioimaging Centre, Mount Sinai Hospital, Pathology & Laboratory Medicine), Dr. Yunfeng Liu, Dr. Lihua Li and Sobia Sultan for their technical support and Dr. Emma Allister for her comments on the manuscript

## Abbreviations

<b>ZnT8</b>	zinc transport family member 8
<b>OGTT</b>	oral glucose tolerance test
<b>TEM</b>	transmission electron microscopy
<b>ZnT8KO</b>	ZnT8 global knockout

<b>ZnT8BKO</b>	ZnT8 beta cell specific knockout
<b>ZnT8AKO</b>	ZnT8 alpha cell specific knockout
<b>PC</b>	prohormone convertase
<b>qPCR</b>	quantitative real time PCR
<b>RIP</b>	rat insulin promoter
<b>KRB</b>	Kreb's ringer buffer
<b>CpE</b>	carboxypeptidase E

## References

- [1]. Sladek R, Rocheleau G, Rung J, et al. A genome-wide association study identifies novel risk loci for type 2 diabetes. *Nature*. 2007; 445:881–885. [PubMed: 17293876]
- [2]. Saxena R, Voight BF, Lyssenko V, et al. Genome-wide association analysis identifies loci for type 2 diabetes and triglyceride levels. *Science*. 2007; 316:1331–1336. [PubMed: 17463246]
- [3]. Scott LJ, Mohlke KL, Bonnycastle LL, et al. A genome-wide association study of type 2 diabetes in Finns detects multiple susceptibility variants. *Science*. 2007; 316:1341–1345. [PubMed: 17463248]
- [4]. Zeggini E, Weedon MN, Lindgren CM, et al. Replication of genome-wide association signals in UK samples reveals risk loci for type 2 diabetes. *Science*. 2007; 316:1336–1341. [PubMed: 17463249]
- [5]. Steinthorsdottir V, Thorleifsson G, Reynisdottir I, et al. A variant in CDKAL1 influences insulin response and risk of type 2 diabetes. *Nat Genet*. 2007; 39:770–775. [PubMed: 17460697]
- [6]. Wenzlau JM, Juhl K, Yu L, et al. The cation efflux transporter ZnT8 (Slc30A8) is a major autoantigen in human type 1 diabetes. *Proc Natl Acad Sci U S A*. 2007; 104:17040–17045. [PubMed: 17942684]
- [7]. Staiger H, Machicao F, Stefan N, et al. Polymorphisms within novel risk loci for type 2 diabetes determine beta-cell function. *PLoS One*. 2007; 2:e832. [PubMed: 17786204]
- [8]. Cauchi S, Proenca C, Choquet H, et al. Analysis of novel risk loci for type 2 diabetes in a general French population: the D.E.S.I.R. study. *J Mol Med*. 2008; 86:341–348. [PubMed: 18210030]
- [9]. Emdin SO, Dodson GG, Cutfield JM, et al. Role of zinc in insulin biosynthesis. Some possible zinc-insulin interactions in the pancreatic B-cell. *Diabetologia*. 1980; 19:174–182. [PubMed: 6997118]
- [10]. Chimienti F, Devergnas S, Pattou F, et al. In vivo expression and functional characterization of the zinc transporter ZnT8 in glucose-induced insulin secretion. *J Cell Sci*. 2006; 119:4199–4206. [PubMed: 16984975]
- [11]. Chimienti F, Devergnas S, Favier A, et al. Identification and cloning of a beta-cell-specific zinc transporter, ZnT-8, localized into insulin secretory granules. *Diabetes*. 2004; 53:2330–2337. [PubMed: 15331542]
- [12]. Lemaire K, Ravier MA, Schraenen A, et al. Insulin crystallization depends on zinc transporter ZnT8 expression, but is not required for normal glucose homeostasis in mice. *Proc Natl Acad Sci U S A*. 2009; 106:14872–14877. [PubMed: 19706465]
- [13]. Nicolson TJ, Bellomo EA, Wijesekara N, et al. Insulin storage and glucose homeostasis in mice null for the granule zinc transporter ZnT8 and studies of the type 2 diabetes-associated variants. *Diabetes*. 2009; 58:2070–2083. [PubMed: 19542200]
- [14]. Pound LD, Sarkar SA, Benninger RK, et al. Deletion of the mouse Slc30a8 gene encoding zinc transporter-8 results in impaired insulin secretion. *Biochem J*. 2009; 421:371–376. [PubMed: 19450229]

- [15]. Seve M, Chimienti F, Devergnas S, et al. In silico identification and expression of SLC30 family genes: an expressed sequence tag data mining strategy for the characterization of zinc transporters' tissue expression. *BMC Genomics*. 2004; 5:32. [PubMed: 15154973]
- [16]. Smidt K, Pedersen SB, Brock B, et al. Zinc-transporter genes in human visceral and subcutaneous adipocytes: lean versus obese. *Mol Cell Endocrinol*. 2007; 264:68–73. [PubMed: 17118530]
- [17]. Overbeck S, Uciechowski P, Ackland ML, et al. Intracellular zinc homeostasis in leukocyte subsets is regulated by different expression of zinc exporters ZnT-1 to ZnT-9. *J Leukoc Biol*. 2008; 83:368–380. [PubMed: 17971500]
- [18]. Murgia C, Devirgiliis C, Mancini E, et al. Diabetes-linked zinc transporter ZnT8 is a homodimeric protein expressed by distinct rodent endocrine cell types in the pancreas and other glands. *Nutr Metab Cardiovasc Dis*. 2009; 19:431–439. [PubMed: 19095428]
- [19]. Gyulkhandanyan AV, Lu H, Lee SC, et al. Investigation of transport mechanisms and regulation of intracellular Zn<sup>2+</sup> in pancreatic alpha-cells. *J Biol Chem*. 2008; 283:10184–10197. [PubMed: 18250168]
- [20]. Egefjord L, P A, Rungby J. Zinc, alpha cells and glucagon secretion. *Current Diabetes Reviews*. 2010; 6
- [21]. Souza SC, Qiu L, Inouye KE, et al. Zinc transporter ZnT-8 regulates insulin and glucagon secretion in Min6 and aTC1-9 pancreatic cell lines. *EASD*. 2009
- [22]. Zhou H, Zhang T, Harmon JS, et al. Zinc, not insulin, regulates the rat alpha-cell response to hypoglycemia in vivo. *Diabetes*. 2007; 56:1107–1112. [PubMed: 17317764]
- [23]. Franklin I, Gromada J, Gjinovci A, et al. Beta-cell secretory products activate alpha-cell ATP-dependent potassium channels to inhibit glucagon release. *Diabetes*. 2005; 54:1808–1815. [PubMed: 15919803]
- [24]. Ishihara H, Maechler P, Gjinovci A, et al. Islet beta-cell secretion determines glucagon release from neighbouring alpha-cells. *Nat Cell Biol*. 2003; 5:330–335. [PubMed: 12640462]
- [25]. Ravier MA, Rutter GA. Glucose or insulin, but not zinc ions, inhibit glucagon secretion from mouse pancreatic alpha-cells. *Diabetes*. 2005; 54:1789–1797. [PubMed: 15919801]
- [26]. Nguyen KT, Tajmir P, Lin CH, et al. Essential role of Pten in body size determination and pancreatic beta-cell homeostasis in vivo. *Mol Cell Biol*. 2006; 26:4511–4518. [PubMed: 16738317]
- [27]. Quoix N, Cheng-Xue R, Guiot Y, et al. The GluCre-ROSA26EYFP mouse: a new model for easy identification of living pancreatic alpha-cells. *FEBS Lett*. 2007; 581:4235–4240. [PubMed: 17706201]
- [28]. Lee SC, Robson-Doucette CA, Wheeler MB. Uncoupling protein 2 regulates reactive oxygen species formation in islets and influences susceptibility to diabetogenic action of streptozotocin. *J Endocrinol*. 2009; 203:33–43. [PubMed: 19635759]
- [29]. O'Gorman D, Kin T, Murdoch T, et al. The standardization of pancreatic donors for islet isolations. *Transplantation*. 2005; 80:801–806. [PubMed: 16210968]
- [30]. Hardy AB, Fox JE, Giglou PR, et al. Characterization of Erg K<sup>+</sup> channels in alpha- and beta-cells of mouse and human islets. *J Biol Chem*. 2009; 284:30441–30452. [PubMed: 19690348]
- [31]. Tam P, Mahfoud R, Nutikka A, et al. Differential intracellular transport and binding of verotoxin 1 and verotoxin 2 to globotriaosylceramide-containing lipid assemblies. *J Cell Physiol*. 2008; 216:750–763. [PubMed: 18446787]
- [32]. Michael J, Carroll R, Swift HH, et al. Studies on the molecular organization of rat insulin secretory granules. *J Biol Chem*. 1987; 262:16531–16535. [PubMed: 3316221]
- [33]. Gyulkhandanyan AV, Lee SC, Bikopoulos G, et al. The Zn<sup>2+</sup>-transporting pathways in pancreatic beta-cells: a role for the L-type voltage-gated Ca<sup>2+</sup> channel. *J Biol Chem*. 2006; 281:9361–9372. [PubMed: 16407176]
- [34]. Tamaki M, Fujitani Y, Uchida T, et al. Downregulation of ZnT8 expression in pancreatic b-cells of diabetic mice. *Islets*. 2009; 1:124–128. [PubMed: 21099260]
- [35]. Fu Y, Tian W, Pratt EB, et al. Down-regulation of ZnT8 expression in INS-1 rat pancreatic beta cells reduces insulin content and glucose-inducible insulin secretion. *PLoS One*. 2009; 4:e5679. [PubMed: 19479076]

- [36]. Rutter GA. Think zinc: new roles for zinc in the control of insulin secretion. *Islets*. 2010; 2:1–2. [PubMed: 21099287]
- [37]. Kahn BB, Flier JS. Obesity and insulin resistance. *J Clin Invest*. 2000; 106:473–481. [PubMed: 10953022]
- [38]. Leung K, Munck A. Peripheral actions of glucocorticoids. *Annu Rev Physiol*. 1975; 37:245–272. [PubMed: 235876]
- [39]. Gromada J, Franklin I, Wollheim CB. Alpha-cells of the endocrine pancreas: 35 years of research but the enigma remains. *Endocr Rev*. 2007; 28:84–116. [PubMed: 17261637]
- [40]. Dodson G, Steiner D. The role of assembly in insulin's biosynthesis. *Curr Opin Struct Biol*. 1998; 8:189–194. [PubMed: 9631292]
- [41]. Kataoka K, Han SI, Shioda S, et al. MafA is a glucose-regulated and pancreatic beta-cell-specific transcriptional activator for the insulin gene. *J Biol Chem*. 2002; 277:49903–49910. [PubMed: 12368292]
- [42]. Ohlsson H, Karlsson K, Edlund T. IPF1, a homeodomain-containing transactivator of the insulin gene. *Embo J*. 1993; 12:4251–4259. [PubMed: 7901001]
- [43]. Kambe T, Narita H, Yamaguchi-Iwai Y, et al. Cloning and characterization of a novel mammalian zinc transporter, zinc transporter 5, abundantly expressed in pancreatic beta cells. *J Biol Chem*. 2002; 277:19049–19055. [PubMed: 11904301]
- [44]. Steiner DF, Rouille Y, Gong Q, et al. The role of prohormone convertases in insulin biosynthesis: evidence for inherited defects in their action in man and experimental animals. *Diabetes Metab*. 1996; 22:94–104. [PubMed: 8792089]
- [45]. Goodge KA, Hutton JC. Translational regulation of proinsulin biosynthesis and proinsulin conversion in the pancreatic beta-cell. *Semin Cell Dev Biol*. 2000; 11:235–242. [PubMed: 10966857]
- [46]. Furuta M, Carroll R, Martin S, et al. Incomplete processing of proinsulin to insulin accompanied by elevation of Des-31,32 proinsulin intermediates in islets of mice lacking active PC2. *J Biol Chem*. 1998; 273:3431–3437. [PubMed: 9452465]
- [47]. Naggert JK, Fricker LD, Varlamov O, et al. Hyperproinsulinaemia in obese fat/fat mice associated with a carboxypeptidase E mutation which reduces enzyme activity. *Nat Genet*. 1995; 10:135–142. [PubMed: 7663508]
- [48]. Yang Y, Chang BH, Samson SL, et al. The Kruppel-like zinc finger protein Glis3 directly and indirectly activates insulin gene transcription. *Nucleic Acids Res*. 2009; 37:2529–2538. [PubMed: 19264802]
- [49]. Eto K, Kaur V, Thomas MK. Regulation of insulin gene transcription by the immediate-early growth response gene Egr-1. *Endocrinology*. 2006; 147:2923–2935. [PubMed: 16543365]
- [50]. Kirchoff K, Machicao F, Haupt A, et al. Polymorphisms in the TCF7L2, CDKAL1 and SLC30A8 genes are associated with impaired proinsulin conversion. *Diabetologia*. 2008; 51:597–601. [PubMed: 18264689]

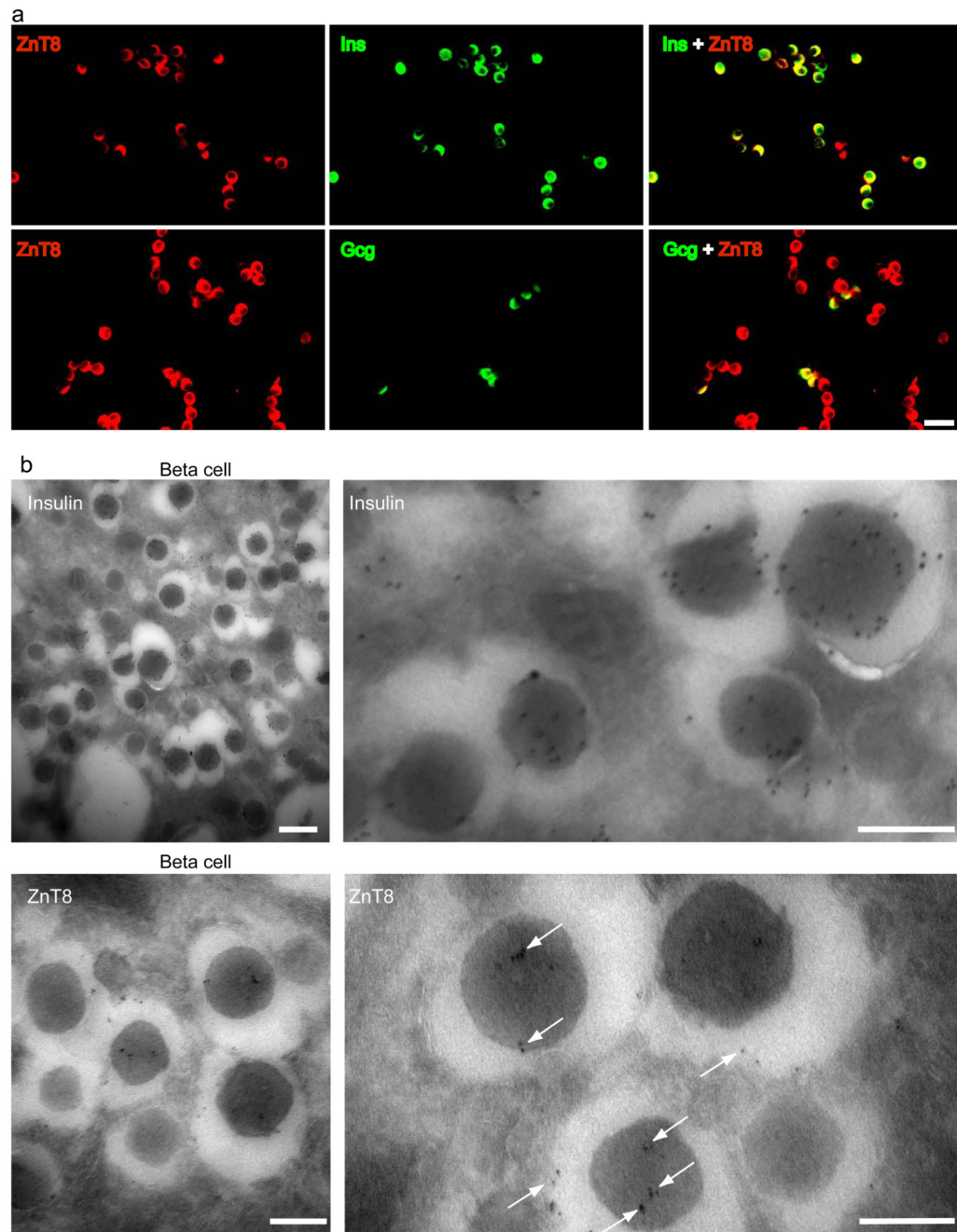


**Figure 1. ZnT8 expression in beta and alpha cells of mouse islets.**

**a.** Dispersed islet cells were immunostained for ZnT8 (red) and insulin (green) [upper panel] or glucagon (green) [lower panel]. Yellow on merged images indicates colocalization of ZnT8 and insulin or glucagon. Scale bar: 20  $\mu$ m. **b.** Electron micrographs of immuno-gold labelled insulin [upper panel] and ZnT8 (arrows) [lower panel] in mouse islet cells. Scale bar: 400 nm [left panels]; 200 nm [right panels].

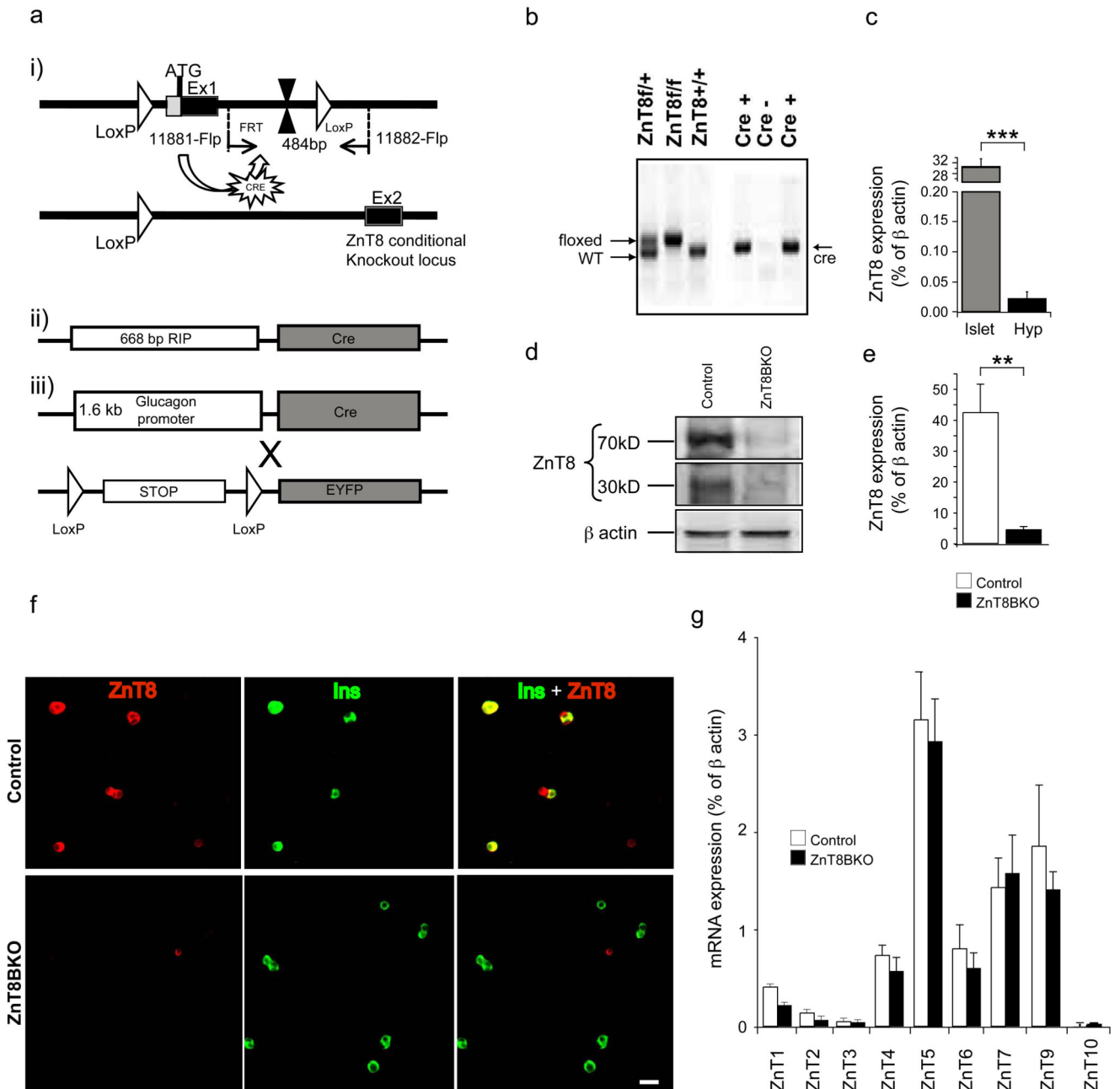


**Figure 2. Generation of ZnT8BKO and ZnT8AKO mice.**

**a.** Schematic diagram of the targeting construct for the ZnT8 gene showing the i) floxed region, ii) RIP-cre and iii) Gcg-cre-YFP transgene constructs. **b.** PCR results of genotyping from tail biopsies of loxP and RIP-cre mice. **c.** qPCR analysis of ZnT8 in wild type mouse islets and hypothalamus (n=3-9, \*\*\*p<0.001). **d.** Western blot and **e.** qPCR analysis of ZnT8 expression in isolated islets from control and ZnT8BKO mice (n=5, \*\*p<0.01). **f.** Dispersed islets from control and ZnT8BKO mice were immuno-stained for ZnT8 (red) and insulin (green). Yellow on merged images indicates colocalization of ZnT8 and insulin. Scale bar:

20  $\mu$ m. g. qPCR analysis of other ZnT transporters in isolated islets from control and ZnT8BKO mice (n=4).

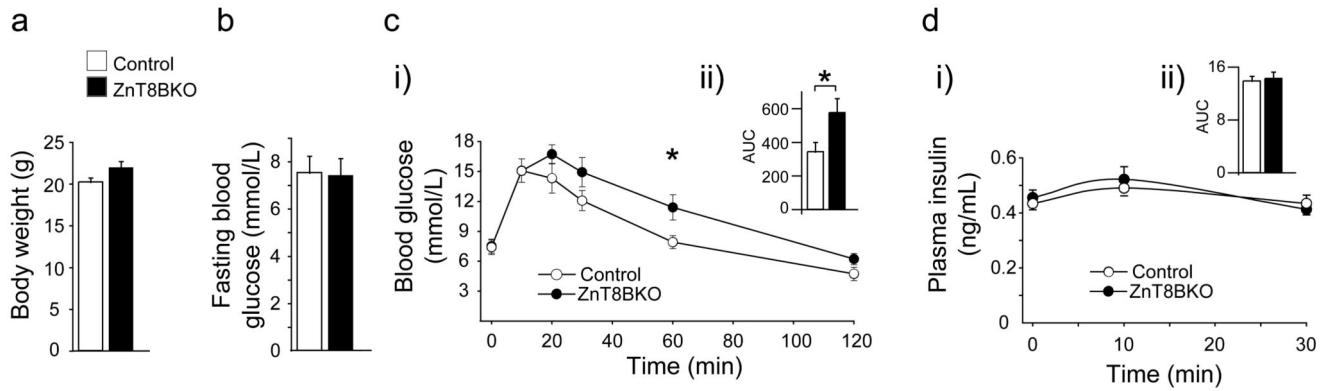


**Figure 3. *In vivo* characterization of ZnT8BKO mice.**

**a.** Body weight, **b.** 6-h fasting blood glucose, and **c.** blood glucose (inset shows the area under the glucose curve) (\* $p < 0.05$ ) and **d.** plasma insulin during OGTT (inset shows the area under the insulin curve) (1.5 g/kg body weight) in 6-week-old control and ZnT8BKO mice ( $n=11$ ).



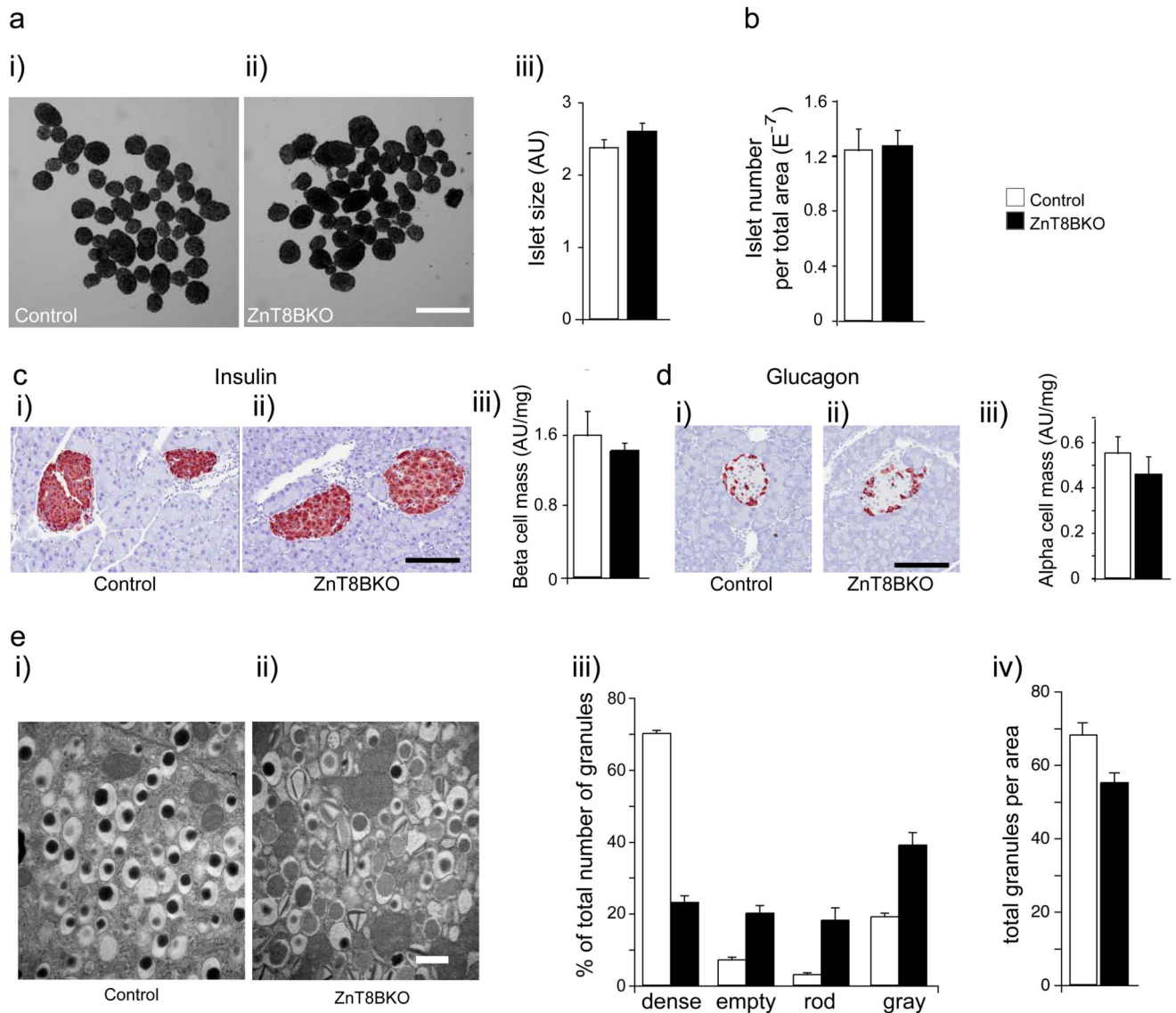


**Figure 4. Islet and beta cell morphological analysis in ZnT8BKO mice.**

**a.** Islet size ( $\mu\text{m}^2$ ) (i. and ii. show representative images of isolated islets from control and ZnT8BKO mice; scale bar: 500  $\mu\text{m}$ ). **b.** islet number per pancreatic slice area (total pixel count). **c.** beta cell mass (i. and ii. show representative images of insulin staining; scale bar: 200  $\mu\text{m}$ ) and **d.** alpha cell mass (i. and ii. show representative images of glucagon staining; scale bar: 200  $\mu\text{m}$ ) in islets from control and ZnT8BKO mice (AU: area unit; n=2). **e.** Electron micrographs of isolated islets from control and ZnT8BKO mice. Manual quantifications were performed on 20 sections from 5 islets per mouse (n=2, scale bar: 500 nm).

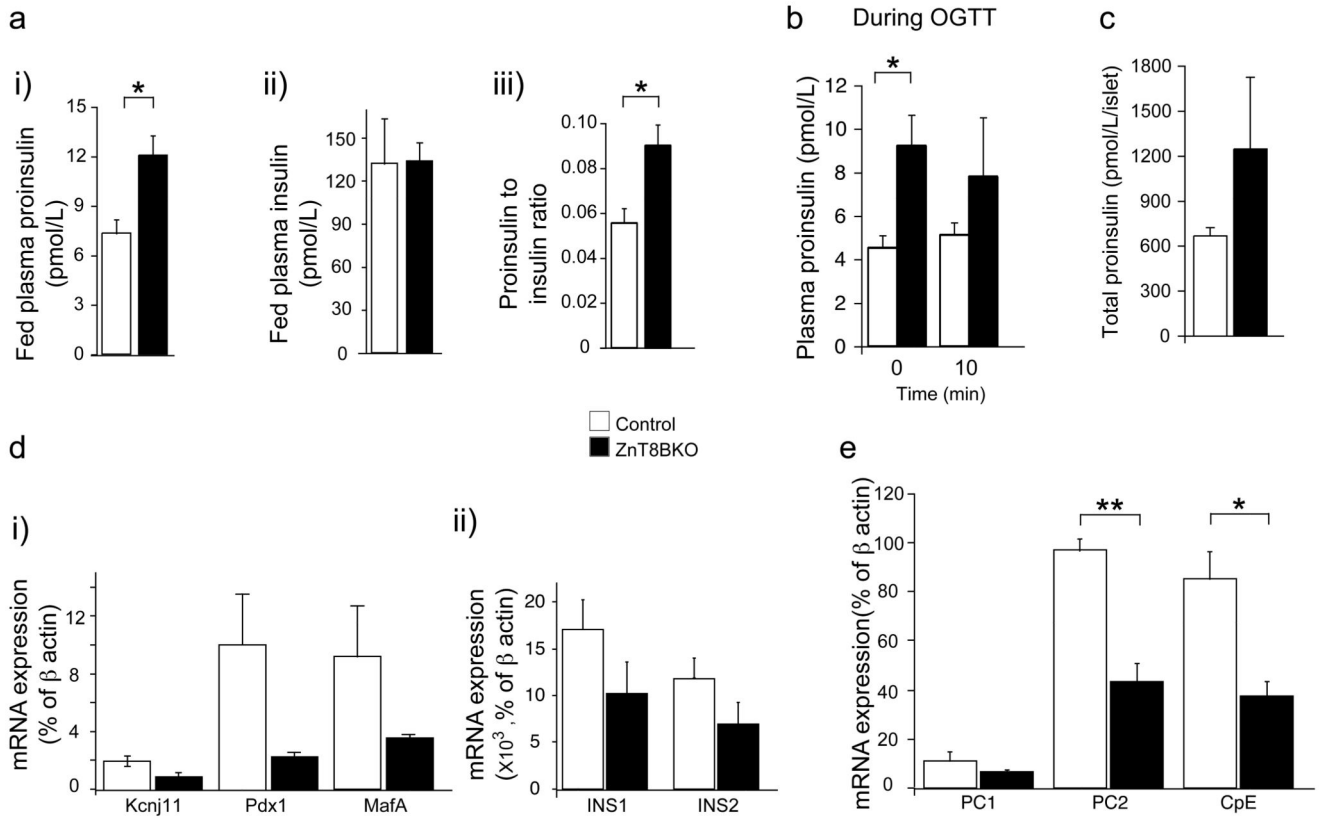


**Figure 5. Analysis of insulin processing in ZnT8BKO mice.**

**a.** Fed plasma proinsulin (i), insulin (ii) and proinsulin to insulin ratio (iii) (n=4, \*p<0.05), **b.** plasma proinsulin during OGTT (1.5 g/kg body weight) (n=4 \*p<0.05), **c.** total proinsulin content per islet (n=4). **d.** mRNA expression of *kcnj11*, *insulin 1* (INS1), *insulin 2* (INS2), *Pdx1* and *MafA* (n=3), **e.** mRNA expression of *prohormone convertase 1* (PC1), *prohormone convertase 2* (PC2) and *carboxypeptidase* (CpE) in islets (n=3, \*\*p<0.01, \*p<0.05) from control and ZnT8BKO mice.

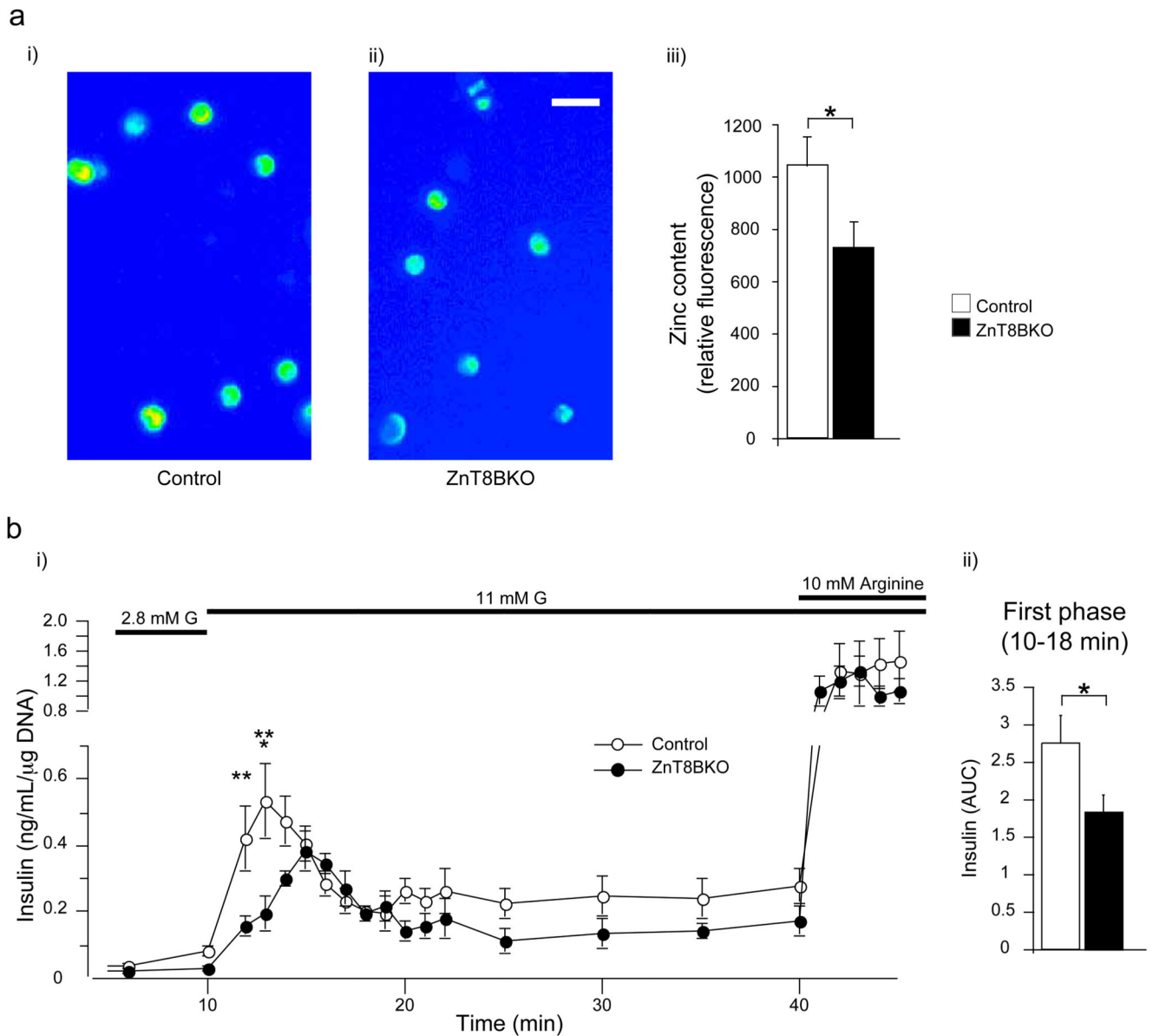


**Figure 6. Intracellular zinc content and *in vitro* insulin secretion from ZnT8BKO islets.**  
**a.** Intracellular zinc content as estimated by zinquin (n=3, \*p<0.05) (i and ii show representative images of dispersed islet cells loaded with zinquin; scale bar: 10  $\mu$ m) and **b.** insulin secretion from isolated islets during perfusion of 2.8 or 11 mM glucose with or without 10 mM arginine (ii shows the area under the glucose curve from 10 to 18 min) (n=4, \*p<0.05, \*\*p<0.01, \*\*\*p<0.001) from control and ZnT8BKO mice.

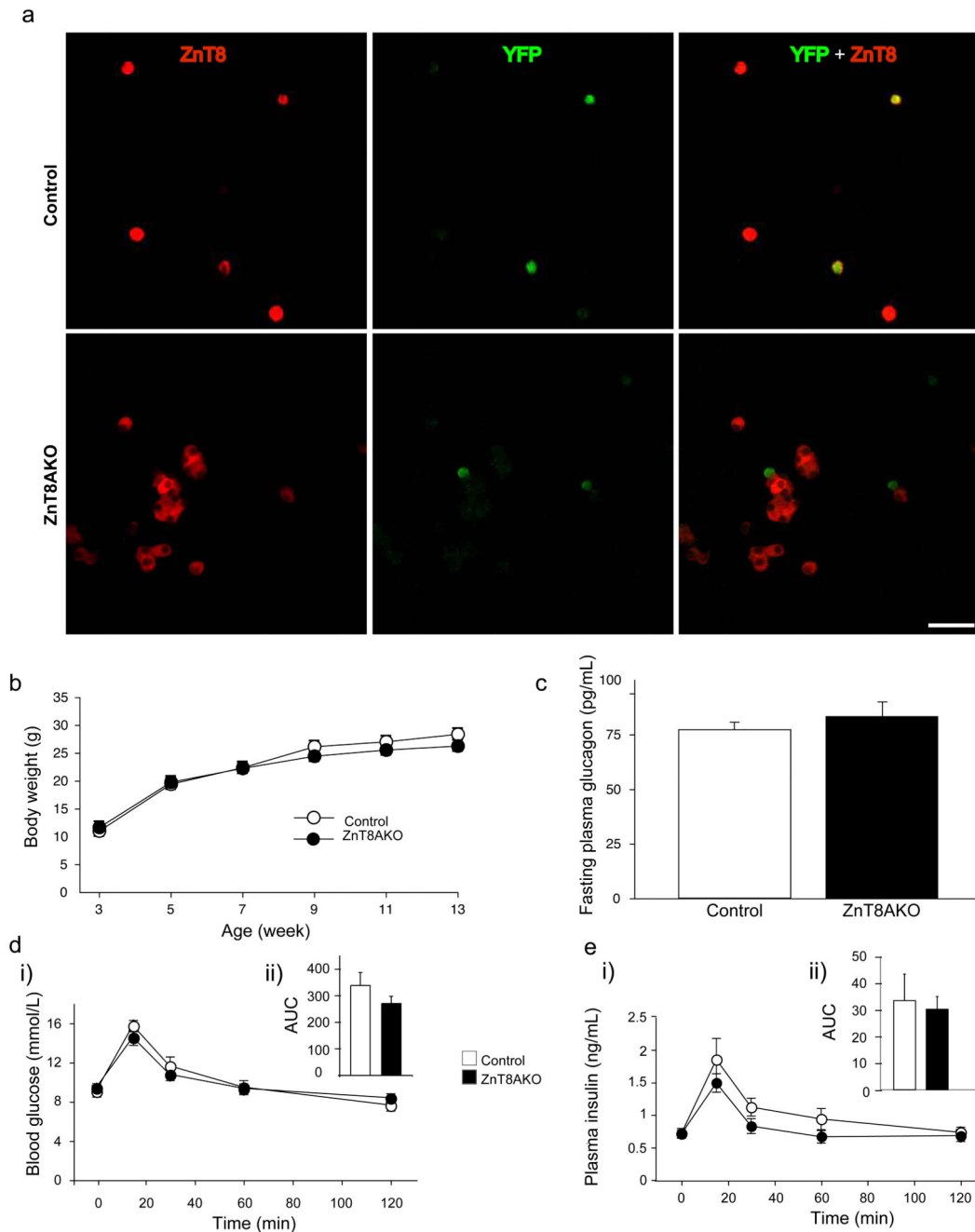


**Figure 7. Characterization of ZnT8AKO mice.**

**a.** Dispersed islets from control and ZnT8AKO mice were immuno-stained for ZnT8 (red) and YFP (green). Yellow on merged images indicates colocalization of ZnT8 and YFP (scale bar: 20  $\mu$ m). **b.** Body weight accumulation, **c.** 16-h fasting plasma glucagon (n=10), and **d.** blood glucose (inset shows the area under the glucose curve) and **e.** plasma insulin during OGTT (inset shows the area under the insulin curve) (2g/kg body weight) in 10 week old control and ZnT8AKO mice (n=5-8).

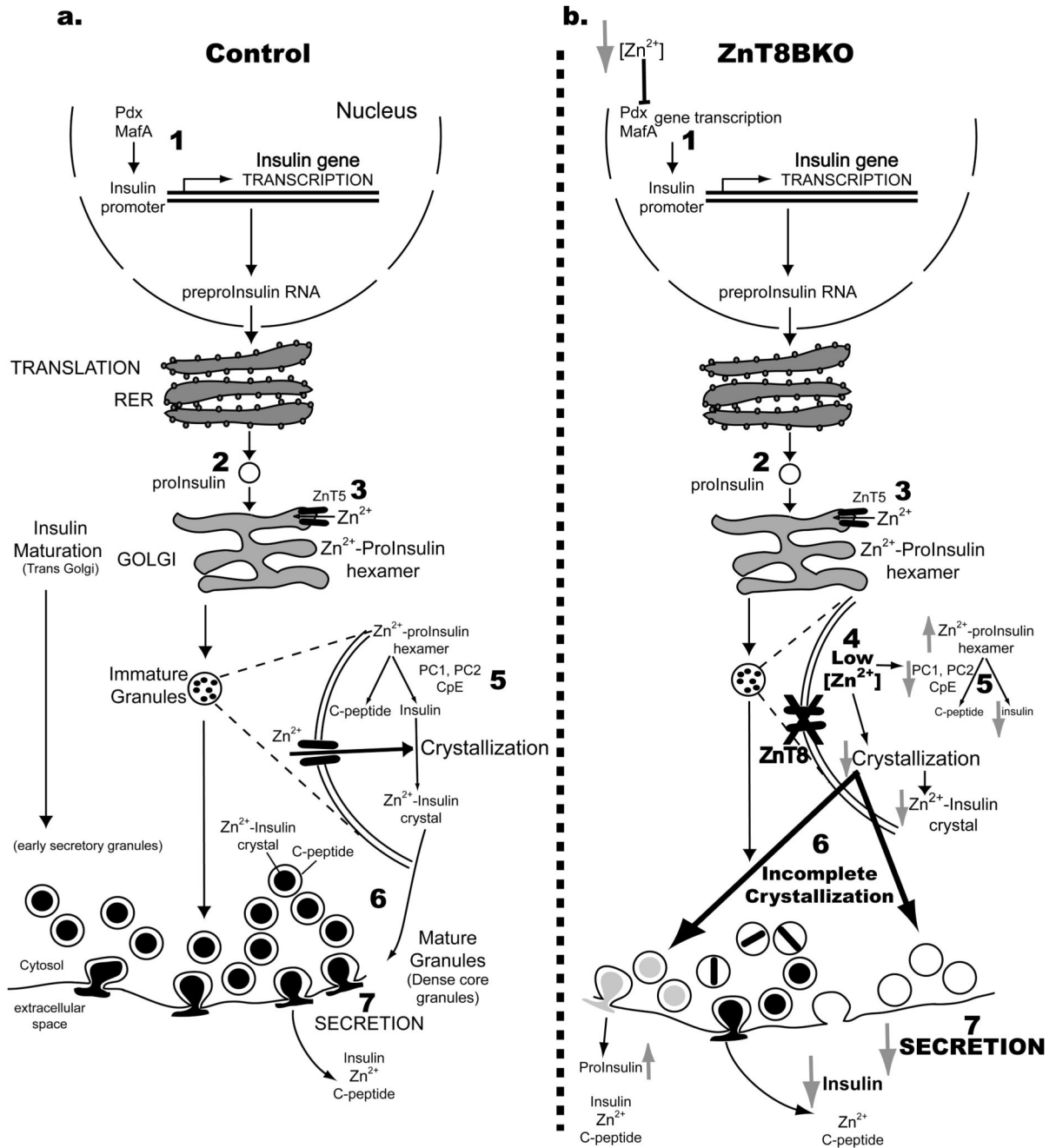


**Figure 8. Role of ZnT8 and zinc in insulin biosynthesis and secretion in control and ZnT8BKO mouse beta cells.**

**1.** Insulin transcription mediated via transcription factors such as PDX1 and MafA. **2.** Proinsulin synthesis. **3.** Zinc-proinsulin hexamerization. **4.** ZnT8 is the primary zinc transporter on insulin granules and its loss in ZnT8BKO beta cells reduces zinc content. **5.** Proinsulin to insulin conversion catalysed by PC1, PC2 and CpE enzymes. Enzyme expression is reduced in ZnT8BKO beta cells, increasing proinsulin content. **6.** Generation of dense core granules following insulin crystallization. Reduced zinc-insulin crystallization,

increased immature, abnormal and empty granules in ZnT8BKO beta cells was observed. **7.** Release of insulin and zinc during granule exocytosis. ZnT8BKO beta cells show reduced insulin secretion and increased proinsulin secretion. ↑ increase, ↓ decrease, ⊥ inhibition